

AeM SERIES No. 2

Proceedings of the 2017 WMO Aeronautical Meteorology Scientific Conference

Commission for Aeronautical Meteorology
assisted by
Commission for Atmospheric Sciences
and
Commission for Basic Systems

Toulouse, France
6–10 November 2017

WEATHER CLIMATE WATER



WORLD
METEOROLOGICAL
ORGANIZATION

Proceedings of the 2017 WMO Aeronautical Meteorology Scientific Conference

Commission for Aeronautical Meteorology
assisted by
Commission for Atmospheric Sciences
and
Commission for Basic Systems

Toulouse, France
6–10 November 2017

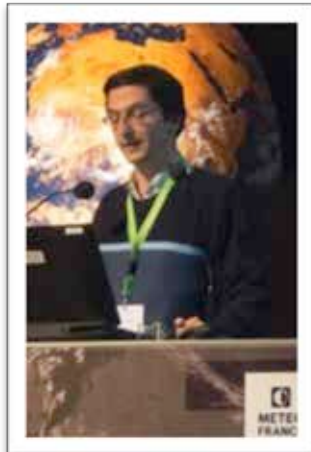


GLOBAL RESPONSE OF CLEAR-AIR TURBULENCE TO CLIMATE CHANGE

By P. Williams, L. Storer and M. Joshi

(Presented by P. Williams)

[Presentation](#)



Introduction

Clear-air turbulence (CAT) is defined as high-altitude aircraft bumpiness in regions devoid of significant cloudiness and away from thunderstorm activity (Chambers, 1955). Without warning, aircraft can be violently thrown about by CAT. Any unsecured objects and unbuckled passengers and crew can be tossed around the cabin, causing serious injuries and even fatalities (De Villiers & van Heerden, 2001). The part of the flight most prone to injuries from CAT is the cruising phase above 10,000 ft, because passengers and crew are often unbuckled (Sharman et al., 2006). Despite recent advances in our mechanistic understanding (Knox et al., 2008; McCann et al., 2012), CAT remains one of the largest causes of weather-related aviation accidents. CAT has been found to account for

24% of weather-related accidents (Kim & Chun, 2011) and turbulence more generally for 65% of weather-related accidents (Sharman et al., 2006). According to official statistics, around 45 passengers and crew are injured by turbulence on United States-operated airlines each year, although these injury rates may be grossly underestimated because not all injuries are reported (Sharman et al., 2006). Turbulence is by far the most common cause of serious injuries to flight attendants (Tvaryanas, 2003).

An important source of CAT is strong vertical wind shear, which is prevalent especially within the atmospheric jet streams. The wind shear creates regions of low Richardson number (Ri), in which unstable Kelvin–Helmholtz waves can grow and ultimately break down into turbulence (Lane et al., 2012). There are several other important sources of CAT, including airflow over mountainous terrain (Lilly, 1978), the effects of remote convection (Koch & Dorian, 1988; Uccellini & Koch, 1987), and loss of balance (Williams et al., 2003, 2005, 2008). In these cases, gravity waves are formed and may propagate far away from the source region, eventually producing turbulence remotely when they either break or induce shear instabilities.

Our current understanding of the response of CAT to climate change has been summarized by Williams and Joshi (2016) and is part of a package of work being carried out in the burgeoning research area of climate impacts on aviation (e.g., Coffel & Horton, 2015; Irvine et al., 2016; Karnauskas et al., 2011; Williams, 2016, 2017; Williams & Joshi, 2013). In particular, Williams and Joshi (2013) used climate model simulations to diagnose 21 different CAT indices and thereby study how a doubling of the atmospheric carbon dioxide (CO_2) concentration could impact the amount of CAT on transatlantic flights in winter at 200 hPa. The north Atlantic flight corridor is one of the busiest in the world, with more than 300 flights per day in each direction (Irvine et al., 2013). From the 21-member ensemble of CAT indices, Williams and Joshi (2013) calculated a 10–40% increase in the median strength of CAT and a 40–170% increase in the frequency of occurrence of MOG CAT in this region, in the doubled- CO_2 simulation compared to a preindustrial control run. This was the first study to calculate how climate change may impact CAT in the future. Williams (2017) subsequently extended the

calculations to study the individual responses of light, moderate, and severe turbulence, finding large and significant increases in each case.

Storer et al. (2017) have recently built on these previous studies by using a current-generation climate model to calculate for the first time how the various strength categories of CAT are projected to change in different geographic regions across the globe, at multiple flight levels, and in all seasons. This extended abstract describes the study by Storer et al. (2017).

Methodology

We use climate simulations that were performed with the Met Office Hadley Centre HadGEM2-ES model (Jones et al., 2011), which forms part of the fifth Coupled Model Inter-comparison Project (CMIP5) ensemble (Taylor et al., 2012). This is the only CMIP5 model for which 6-hourly output fields have been archived on a suitable set of upper-tropospheric and lower-stratospheric pressure levels. The 6-hourly snapshots resolve the diurnal cycle and are therefore expected to provide a better representation of wind shear than the daily mean CMIP3 fields used by Williams and Joshi (2013) and Williams (2017). The multiple pressure levels make it possible to calculate the vertical wind shear using second-order centered finite differences at both 200 hPa and 250 hPa, which correspond to typical cruising altitudes of approximately 12 km (39,000 ft or FL390) and 10 km (34,000 ft or FL340), respectively. The atmosphere model has a horizontal grid spacing of 1.25° in latitude and 1.875° in longitude, giving 192 × 144 grid boxes globally, which is finer than the 2.0° by 2.5° CMIP3 model used by Williams and Joshi (2013) and Williams (2017).

Two HadGEM2-ES simulations are analysed to calculate how climate change could impact CAT in the upper troposphere and lower stratosphere in future. Specifically, a preindustrial control simulation (picontrol) is compared with a climate change simulation using the Intergovernmental Panel on Climate Change (IPCC) Representative Concentration Pathway 8.5 (RCP8.5) (Flato et al., 2013). The picontrol run is a base state that uses constant preindustrial greenhouse gas concentrations to simulate the global climate before the industrial revolution. The RCP8.5 run assumes a net radiative forcing increase of 8.5 W m⁻² by 2100 (Van Vuuren et al., 2011), which implies greenhouse gas concentrations equivalent to around 1,370 ppmv of CO₂. We analyse 30 years of data for the future period 2050–2080 from RCP8.5 compared to 30 years of historic data from picontrol.

The present study focuses on CAT generated by wind shear and loss of balance, disregarding mountain waves and remote convection. For consistency, we calculate the same basket of CAT diagnostics indices as Williams and Joshi (2013) and Williams (2017), except that we exclude the potential vorticity diagnostic because it was found to give unrealistic results. We define a threshold for each turbulence strength category and each CAT diagnostic in HadGEM2-ES, following Williams (2017); see Storer et al. (2017) for full details.

Results

Global geographic maps of the percentage change in the prevalence of moderate turbulence in the HadGEM2-ES simulations at 200 hPa in December, January, and February (DJF) are shown in Figure 1 for each of the 20 CAT indices. The percentage change refers to the period 2050–2080 compared to preindustrial times. The indices are ranked in descending order according to the global-mean percentage change. (All geographic averages in this paper include the cosine (latitude) scaling factor, to down-weight the smaller high-latitude grid boxes compared to the larger low-latitude ones.) Previous findings about CAT increasing in the North Atlantic evidently apply to other parts of the planet, too. In the tropical regions (30°S–30°N), the percentage changes are generally smaller and there is less agreement between the diagnostics. Outside the

tropics, in the middle- and high-latitude regions, the percentage changes are generally larger and there is more agreement between the diagnostics.

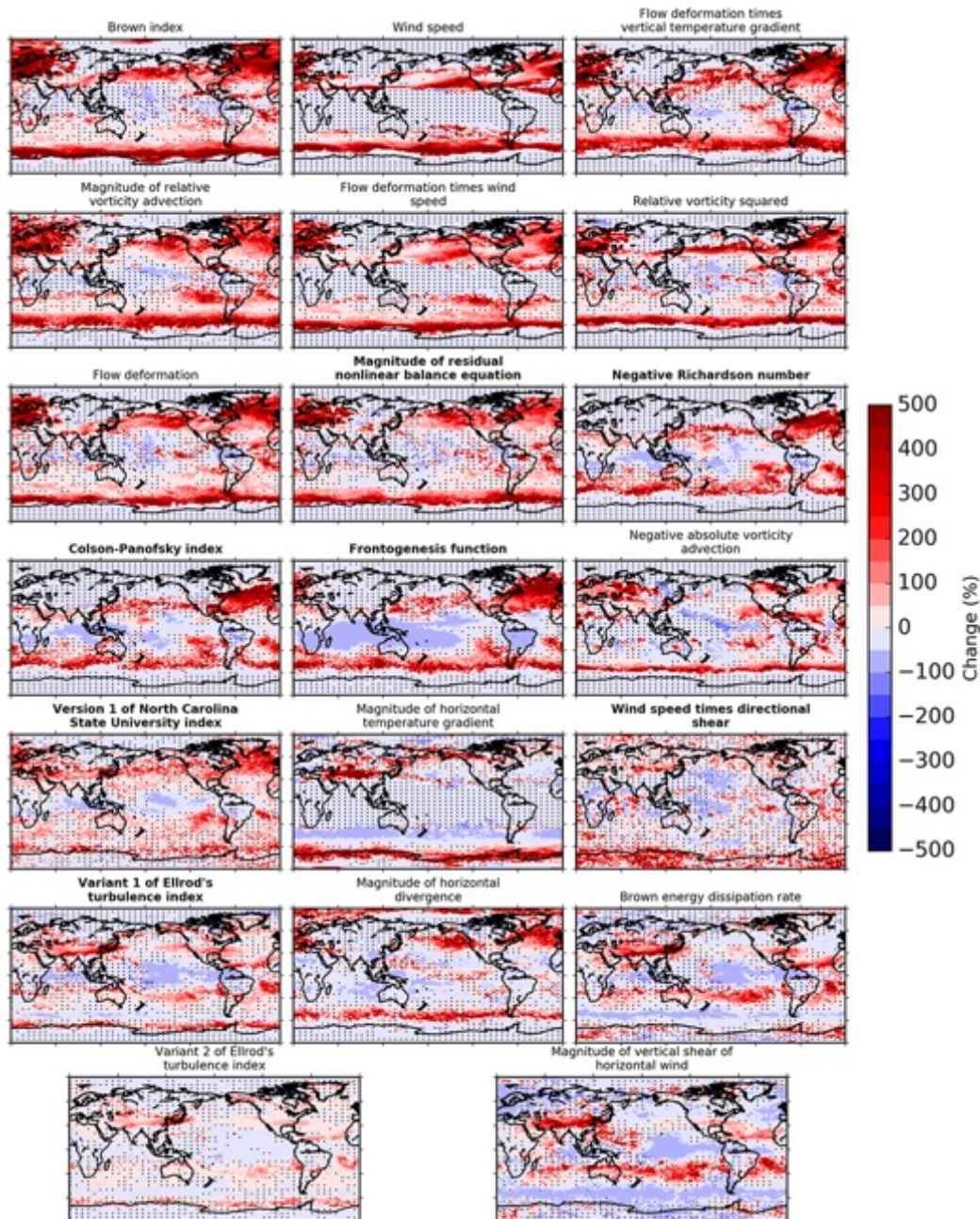


Figure 1. Maps of the percentage change in the amount of moderate CAT from preindustrial times (picontrol) to the period 2050–2080 (RCP8.5). The maps are calculated for all 20 CAT diagnostics at 200 hPa in December, January, and February (DJF) using the HadGEM2-ES climate model. The maps are ordered (from left to right and top to bottom) from the largest to smallest global-mean percentage change. Bold titles indicate the seven GTG2 upper-level diagnostics that are used operationally (Sharman et al., 2006). Stippling indicates regions where the percentage change is not statistically significant at the 90% level according to the two-tailed binomial test.

To assess which features are robust among the different diagnostics, the 20 estimates of the percentage changes in CAT shown in Figure 1 for DJF are averaged and shown in the first panel of Figure 2. The remaining three panels in Figure 2 show the corresponding

averages for March, April, and May (MAM), June, July, and August (JJA), and September, October, and November (SON). The averages being taken here are equally weighted, under the assumption that each of the 20 estimates is equally plausible. The percentage changes generally display relatively little seasonality, with the bulk spatial patterns occurring in all four seasons, although there does appear to be a moderate seasonal amplitude modulation locally in some regions. These bulk changes include large increases of several hundred per cent in the mid-latitudes in both hemispheres. In the Southern Hemisphere, these increases peak at around 45–75°S and are fairly zonally symmetric. In the Northern Hemisphere, the increases peak at around 45–75°N but they display more zonal variability, which appears to be associated with the presence of land masses. The bulk features also include small and statistically insignificant decreases of several tens of per cent in parts of the tropics (where convection is a more important source of turbulence and CAT is less relevant). The global-mean percentage changes in moderate CAT at 200 hPa are +30.8% (DJF), +46.5% (MAM), +42.7% (JJA), and +39.2% (SON), where large increases in the mid-latitudes are being partly offset by small decreases in the tropics.

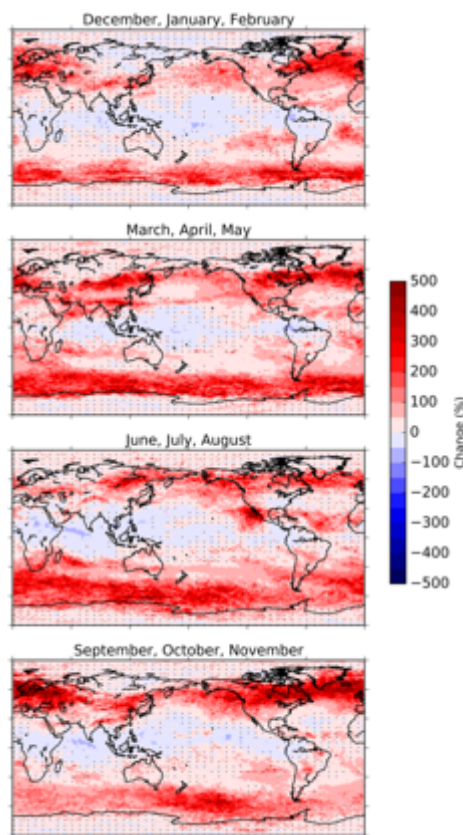


Figure 2. Maps of the average percentage change in the amount of moderate CAT from preindustrial times (picontrol) to the period 2050–2080 (RCP8.5) at 200 hPa in each season. The average is taken over all 20 CAT diagnostics, which are equally weighted. The upper panel for December, January, and February is the average of the 20 panels in Figure 1. Stippling indicates regions where the average percentage change is not significantly different from zero at the 90% level according to the one-sample, two-tailed t test.

The global-mean percentage changes for all five turbulence strength categories (light, light-to-moderate, moderate, moderate-to-severe, and severe) and both pressure levels (200 hPa and 250 hPa) in all four seasons (DJF, MAM, JJA, and SON) are tabulated in Figure 3. In all 40 cases, the change is positive, indicating that CAT is intensifying across a range of strengths and altitudes and that it is intensifying throughout the year. The

global-mean percentage changes are generally larger at 200 hPa than 250 hPa, largest for turbulence in the light strength category, and largest in MAM.

Strength	DJF		MAM		JJA		SON	
Category	200 hPa	250 hPa						
Light	+39.8	+23.2	+53.7	+32.3	+52.6	+31.8	+47.2	+26.6
Light-to-moderate	+35.9	+22.4	+53.4	+31.6	+51.4	+31.2	+45.9	+24.6
Moderate	+30.8	+19.6	+46.5	+30.0	+42.7	+28.3	+39.2	+23.5
Moderate-to-severe	+27.9	+17.5	+42.3	+28.0	+35.4	+25.3	+34.0	+21.4
Severe	+34.7	+20.5	+51.6	+34.2	+42.7	+29.8	+41.9	+25.5

Note. The changes are calculated for five turbulence strength categories, at two pressure altitudes, and in four seasons. The changes are averaged over 20 CAT diagnostics. DJF is December, January, and February; MAM is March, April, and May; JJA is June, July, and August; and SON is September, October, and November.

Figure 3. Global-mean percentage changes in the amount of CAT from pre-industrial times (picontrol) to the period 2050–2080 (RCP8.5).

Because the above global averages mask large regional variations, Figure 4 tabulates the annual-mean percentage changes averaged within eight geographic regions, for all five turbulence strength categories and both pressure levels. The results indicate that the busiest international airspace around the middle and high latitudes (North Atlantic, North America, North Pacific, Europe, and Asia) experiences larger increases in CAT than the global average, with the volume of severe CAT approximately doubling at 200 hPa over North America (+112.7%), the North Pacific (+91.6%), and Europe (+160.7%). The less congested skies around the tropics (Africa, South America, and Australia) generally experience smaller increases. Whereas globally, it is light turbulence that experiences the largest relative increase, locally, it can be severe turbulence (e.g., Europe). For each strength category and geographic region, the percentage change is larger at 200 hPa than 250 hPa. To provide some context to aid with the interpretation of the magnitudes of these changes, in the North Atlantic (50–75°N, 10–60°W) at 200 hPa, we find that (i) in winter, severe CAT by 2050–2080 will be as common as moderate CAT in the control period, and (ii) for a range of turbulence strengths from light to moderate-to-severe, summertime CAT by 2050–2080 will be as common as wintertime CAT in the control period.

Strength	North Atlantic		North America		North Pacific		Europe	
Category	200 hPa	250 hPa	200 hPa	250 hPa	200 hPa	250 hPa	200 hPa	250 hPa
Light	+75.4	+47.3	+110.1	+71.0	+120.7	+82.0	+90.5	+59.9
Light-to-moderate	+124.1	+80.7	+113.6	+57.5	+106.6	+53.8	+130.7	+75.8
Moderate	+143.3	+74.4	+100.3	+50.2	+90.2	+41.6	+126.8	+60.8
Moderate-to-severe	+148.9	+71.0	+94.3	+47.0	+73.1	+35.3	+142.1	+66.1
Severe	+181.4	+88.0	+112.7	+58.9	+91.6	+40.1	+160.7	+90.6
Strength	South America		Africa		Asia		Australia	
Category	200 hPa	250 hPa	200 hPa	250 hPa	200 hPa	250 hPa	200 hPa	250 hPa
Light	+18.3	+13.4	+24.2	+18.9	+102.5	+65.1	+18.0	+9.5
Light-to-moderate	+27.1	+18.0	+27.9	+23.3	+92.4	+48.7	+23.1	+12.9
Moderate	+34.3	+22.8	+34.3	+26.0	+78.1	+48.7	+29.6	+19.1
Moderate-to-severe	+43.3	+23.8	+36.6	+26.9	+59.2	+47.9	+36.9	+24.8
Severe	+62.0	+31.6	+51.1	+40.2	+64.1	+55.4	+52.5	+35.4

Note. The changes are calculated for five turbulence strength categories, at two pressure altitudes, and within eight geographic regions. The changes are averaged over 20 CAT diagnostics. The geographic regions are: North Atlantic (50–75°N, 10–60°W), North America (25–75°N, 63–123°W), North Pacific (50–75°N, 145°E–123°W), Europe (35–75°N, 10°W–30°E), South America (55°S–10°N, 35–80°W), Africa (35°S–35°N, 15°W–50°E), Asia (10–75°N, 45–140°E), and Australia (12–46°S, 113–177°E).

Figure 4: Annual-mean percentage changes in the amount of CAT from pre-industrial times (picontrol) to the period 2050–2080 (RCP8.5).

Summary and Discussion

Using climate model simulations, the study conducted by Storer et al. (2017) and described in this extended abstract found large relative increases in the atmospheric volume containing significant CAT by the period 2050–2080 under the RCP8.5 greenhouse gas forcing scenario. The increases occur throughout the global atmosphere but are most pronounced in the mid-latitudes in both hemispheres. The increases occur in multiple aviation-relevant turbulence strength categories, at multiple flight levels, and in all seasons. We conclude that the intensification of CAT that has been calculated by previous studies, which considered only transatlantic flights in winter at altitudes of around 39,000 feet, apply more generally.

Our findings may have implications for aviation operations in the coming decades. Many of the aircraft that will be flying in the second half of the present century are currently in the design phase. It would therefore seem sensible for the airframe manufacturers to prepare for a more turbulent atmosphere, even at this early stage. Future aeronautical advances, such as remote sensing of clear-air turbulence using on-board light detection and ranging technology, might be able to mitigate the operational effects of the

worsening atmospheric turbulence (Vrancken et al., 2016). Our results also reinforce the increasingly urgent need to improve the skill of operational CAT forecasts. Despite containing useful information and demonstrably improving the safety and comfort of air travel, these forecasts continue to include a substantial fraction of false positives and missed events.

References

- Brown, R., 1973: *New indices to locate clear-air turbulence*. Meteorological Magazine, 102, 347–361.
- Chambers, E., 1955: *Clear air turbulence and civil jet operations*. The Aeronautical Journal, 59(537), 613–628.
- Coffel, E., and R. Horton, 2015: *Climate change and the impact of extreme temperatures on aviation*. Weather, Climate, and Society, 7, 94–102.
- Colson, D., and H. Panofsky, 1965: *An index of clear air turbulence*. Quarterly Journal of the Royal Meteorological Society, 91(390), 507–513.
- De Villiers, M., and J. van Heerden, 2001: *Clear air turbulence over South Africa*. Meteorological Applications, 8(1), 119–126.
- Ellrod, G. P., and D. I. Knapp, 1992: *An objective clear-air turbulence forecasting technique: Verification and operational use*. Weather and Forecasting, 7(1), 150–165.
- Flato, G., J. Marotzke, B. Abiodun, P. Braconnot, S. C. Chou, W. J. Collins, Rummukainen, M., 2013: *Evaluation of climate models*. In T. F. Stocker et al. (Eds.), Climate Change 2013: The Physical Science Basis. Contribution of Working Group I to the Fifth Assessment Report of the Intergovernmental Panel on Climate Change (pp. 741–866). Cambridge, UK: Cambridge University Press.
- Irvine, E. A., K. P. Shine, and M. A. Stringer, 2016: *What are the implications of climate change for trans-Atlantic aircraft routing and flight time?*. Transportation Research Part D: Transport and Environment, 47, 44–53.
- Irvine, E. A., B. J. Hoskins, K. P. Shine, R. W. Lunnon, and C. Froemming, 2013: *Characterizing North Atlantic weather patterns for climate-optimal aircraft routing*. Meteorological Applications, 20(1), 80–93.
- Jaeger, E., and M. Sprenger, 2007: *A Northern Hemispheric climatology of indices for clear air turbulence in the tropopause region derived from ERA40 reanalysis data*. Journal of Geophysical Research: Atmospheres, 112, D20106. <https://doi.org/10.1029/2006JD008189>
- Jones, C., J. Hughes, N. Bellouin, S. Hardiman, G. Jones, J. Knight, M. Zerroukat, 2011: *The HadGEM2-ES implementation of CMIP5 centennial simulations*. Geoscientific Model Development, 4(3), 543–570.
- Karnauskas, K. B., J. P. Donnelly, H. C. Barkley, and J. E. Martin, 2011: *Coupling between air travel and climate*. Nature Climate Change, 5, 1068–1073.
- Kim, J.-H., and H.-Y. Chun, 2011: *Statistics and possible sources of aviation turbulence over South Korea*. Journal of Applied Meteorology and Climatology, 50(2), 311–324.

- Kim, J.-H., W. N. Chan, B. Sridhar, R. D. Sharman, P. D. Williams, & M. Strahan, 2016: *Impact of the North Atlantic Oscillation on transatlantic flight routes and clear-air turbulence*. *Journal of Applied Meteorology and Climatology*, 55(3), 763–771.
- Knox, J. A., D. W. McCann, and P. D. Williams, 2008: *Application of the Lighthill–Ford theory of spontaneous imbalance to clear-air turbulence forecasting*. *Journal of the Atmospheric Sciences*, 65(10), 3292–3304.
- Koch, S. E., and P. B. Dorian, 1988: *A mesoscale gravity wave event observed during CCOPE. Part III: Wave environment and probable source mechanisms*. *Monthly Weather Review*, 116(12), 2570–2592.
- Lane, T. P., R. D. Sharman, S. B. Trier, R. G. Fovell, and J. K. Williams, 2012: *Recent advances in the understanding of near-cloud turbulence*. *Bulletin of the American Meteorological Society*, 93(4), 499–515.
- Lilly, D. K., 1978: *A severe downslope windstorm and aircraft turbulence event induced by a mountain wave*. *Journal of the Atmospheric Sciences*, 35(1), 59–77.
- MacCready, P. B., 1964: *Standardization of gustiness values from aircraft*. *Journal of Applied Meteorology*, 3(4), 439–449.
- McCann, D. W., J. A. Knox, & P. D. Williams, 2012: *An improvement in clear-air turbulence forecasting based on spontaneous imbalance theory: The ULTURB algorithm*. *Meteorological Applications*, 19(1), 71–78.
- Sharman, R., and T. Lane, 2016: *Aviation Turbulence: Processes, Detection, Prediction* (523 pp.). Switzerland: Springer.
- Sharman, R., C. Tebaldi, G. Wiener, and J. Wolff, 2006: *An integrated approach to mid- and upper-level turbulence forecasting*. *Weather and Forecasting*, 21(3), 268–287.
- Storer, L. N., P. D. Williams, and M. M. Joshi, 2017: *Global response of clear-air turbulence to climate change*. *Geophysical Research Letters*, 44.
<https://doi.org/10.1002/2017GL074618>
- Taylor, K. E., R. J. Stouffer, and G. A. Meehl, 2012. *An overview of CMIP5 and the experiment design*. *Bulletin of the American Meteorological Society*, 93(4), 485–498.
- Tvaryanas, A. P., 2003: *Epidemiology of turbulence-related injuries in airline cabin crew, 1992–2001*. *Aviation, Space, and Environmental Medicine*, 74(9), 970–976.
- Uccellini, L. W., and S. E. Koch, 1987: *The synoptic setting and possible energy sources for mesoscale wave disturbances*. *Monthly Weather Review*, 115(3), 721–729.
- Van Vuuren, D. P., J. Edmonds, M. Kainuma, K. Riahi, A. Thomson, K. Hibbard, S. K. Rose, 2011: *The representative concentration pathways: An overview*. *Climatic Change*, 109, 5–31.
- Vrancken, P., M. Wirth, G. Ehret, H. Barny, P. Rondeau, and H. Veerman, 2016: *Airborne forward-pointing UV Rayleigh lidar for remote clear air turbulence detection: System design and performance*. *Applied Optics*, 55(32), 9314–9328.
- Williams, P. D. (2016). *Transatlantic flight times and climate change*. *Environmental Research Letters*, 11(2), 024008.

- Williams, P. D. (2017). *Increased light, moderate, and severe clear-air turbulence in response to climate change*. *Advances in Atmospheric Sciences*, 34(5), 576–586.
- Williams, P. D., and M. M. Joshi, 2013: *Intensification of winter transatlantic aviation turbulence in response to climate change*. *Nature Climate Change*, 3, 644–648.
- Williams, P. D., and M. M. Joshi, 2016: *Clear-air turbulence in a changing climate*. Chapter 23 (pp. 465–480).. In R. Sharman, & T. Lane (Eds.), *Aviation Turbulence: Processes, Detection, Prediction* (523 pp.). Switzerland: Springer.
- Williams, P. D., T. W. N. Haine, and P. L. Read, 2005: *On the generation mechanisms of short-scale unbalanced modes in rotating two-layer flows with vertical shear*. *Journal of Fluid Mechanics*, 528, 1–22.
- Williams, P. D., T. W. N. Haine, and P. L. Read, 2008: *Inertia–gravity waves emitted from balanced flow: Observations, properties, and consequences*. *Journal of the Atmospheric Sciences*, 65(11), 3543–3556.
- Williams, P. D., P. L. Read, & T. W. N. Haine, 2003: *Spontaneous generation and impact of inertia–gravity waves in a stratified, two-layer shear flow*. *Geophysical Research Letters*, 30(24), 2255. <https://doi.org/10.1029/2003GL018498>
-